

# Adaptive Ensemble Biomolecular Simulations at Scale

Vivek Balasubramanian\*, Travis Jensen†, Matteo Turilli\*, Peter Kasson‡, Michael Shirts†, Shantenu Jha\*§

\*Department of ECE, Rutgers University

†Department of ChBE, University of Colorado Boulder

‡Biomedical Engineering, University of Virginia

§Brookhaven National Laboratory

**Abstract**—Recent advances in both theory and methods have created opportunities to simulate biomolecular processes more efficiently using adaptive ensemble simulations. Ensemble-based simulations are used widely to compute a number of individual simulation trajectories and analyze statistics across them. Adaptive ensemble simulations offer a further level of sophistication and flexibility by enabling high-level algorithms to control simulations based on intermediate results. Novel high-level algorithms require sophisticated approaches to utilize the intermediate data during runtime. Thus, there is a need for scalable software systems to support adaptive ensemble-based applications. We describe three different types of adaptations and propose four operations necessary to support these adaptations. We identify and address the challenges of expressibility, instantiation and implementation of the four operations. We enhance the Ensemble Toolkit – an ensemble execution system – with abstractions to support these operations. We characterize the overhead of supporting adaptive capabilities in the toolkit at production scale. We implement two high-level adaptive algorithms: expanded ensemble and Markov state modeling. We highlight scientific advantages enabled by the novel capabilities of our approach and implementation on three distinct platforms.

**Index Terms**—Adaptivity, Ensemble Applications

## I. INTRODUCTION

Current computational methods for solving scientific problems in biomolecular science are at or near their scaling limits using traditional parallel architectures [1]. Computations using straightforward molecular dynamics (MD) are inherently sequential processes, and parallelization is limited to speeding up each individual, serialized, timestep. Consequently, *ensemble-based* computational methods have been developed to address this gap. In these methods, [2]–[5] multiple simulation tasks are executed concurrently, and various physical or statistical principles are used to combine the tasks together with longer time scale communication (seconds to hours) instead of the microsecond to milliseconds required for standard tightly coupled parallel processing.

Existing ensemble-based methods have been successful for addressing a number of questions in biomolecular modeling [6], [7]. However, studying systems with multiple-timescale behavior extending out to microseconds or milliseconds, or studying even shorter timescales on larger physical systems will not only require tools that can support  $100\times$ – $1000\times$  greater degrees of parallelism but also require exploration of *adaptive* algorithms. In adaptive algorithms, the intermediate results of

simulations are used to alter future simulations. Adaptive approaches can increase simulation efficiency by greater than a thousand-fold [8] but require a more sophisticated software infrastructure to support them, in order to encode, modularize, and execute complex interactions and execution logic.

We define *adaptivity* as the capability to change, based on current information available, one or more attributes that influence execution performance or domain specific parameter(s). The logic to specify such changes can rely on a single simulation within an ensemble, an operation across an ensemble, or even external criteria, such as changes in resource availability or new experimental data. In most cases, adaptive algorithms can be expressed at a high level, such that the adaptive logic itself is independent of simulation details (i.e., external to MD kernel). In fact, this separation of adaptive operations from simulation internals provides a useful and important abstraction for both methods developers and software system. Adaptive operations that are expressed independent of the internal details of tasks facilitate MD software package agnosticism and simpler expression of different types of adaptivity and responses to adaptivity. This promotes facile development of new methods while facilitating scalable system software and its optimization and performance engineering.

Adaptivity and automation are critical requirements to study longer simulation durations, investigate larger physical systems and to efficiently explore high dimensional surfaces with rugged fitness landscapes. The execution trajectory of the application cannot be fully determined *a priori*, but depends upon intermediate results. Adaptive algorithms “steer” execution towards interesting phase space or parameters and thus improve sampling quality or sampling rate. To achieve scalability and efficiency, such adaptivity cannot be performed via user intervention and hence automation of the control logic and execution is important.

To guide the design and implementation of capabilities to encode and execute adaptive ensemble applications in a scalable and adaptive manner, we identify two such applications from the biomolecular science domain as schematized in Figs. 1 and 2. Although each of these biomolecular applications have distinct coordination and communication patterns among their ensemble members and execution requirements, they are united by their need for adaptive execution of multiple concurrent tasks.

This paper makes the following contributions:

- analyzes the steps to execute an adaptive application and identifies different types of adaptations
- enhances an ensemble execution system (EnTK) with adaptive capabilities and characterizes the cost of such capabilities
- demonstrates the capability to execute novel adaptive applications at scale and validates the scientific results obtained from these applications

To the best of our knowledge, this is the first time that multiple adaptive ensemble applications have been implemented using a common conceptual and implementation framework. The results and capabilities apply uniformly to adaptive ensemble applications from any domain. This work is being utilized in other domains such as climate science, seismic physics, astrophysics, and uncertainty quantification.

Section II describes existing solutions and their limitations in their ability to support adaptive applications. Section III presents two science drivers that motivate the need for large-scale adaptive biomolecular simulations. We describe adaptive execution, their different types and challenges in supporting adaptivity in Section IV. In Section V, we describe the design and implementation of the EnTK, and the enhancements made to address the challenges of adaptivity. In Section VI, we characterize the overheads in EnTK as a function of the adaptivity types, validate the implementation of the science drivers using EnTK, and discuss the results of executing the expanded ensemble application at production scale.

## II. RELATED WORK

Algorithms consisting of one or more MD simulations, provide quantitative and qualitative information about the structure and stability of molecular systems, and the interactions among them. Specialized computer architectures enable single MD simulations at the millisecond scale [9], [10] but alternative approaches are motivated by the higher availability of general-purpose machines and the need to investigate biological processes at the scales from milliseconds to minutes. Importantly, although we discuss mostly biological applications, there are many applications of molecular dynamics in material science, polymer science, and interface science [11], [12].

Statistical estimation of thermodynamic, kinetic, and structural properties of biomolecules requires multiple samples of biophysical events. MD algorithms with ensembles of MD simulations have been shown to be more efficient at computing these samples [2]–[5]. Further advances in MD algorithms, exhibiting a thousand-fold increase in efficiency [13], [14], have been achieved by executing adaptive ensemble algorithms, where intermediate data are used to guide the progression of simulations.

Building upon these advances, several adaptive ensemble algorithms have been formulated. Replica exchange [15] consists of ensembles of simulations where each simulation operates with a unique value of a sampling parameter, such as temperature, to facilitate escape from local minima. In generalized ensemble simulation methods, different ensemble members

employ different exchange algorithms [16] or specify different sampling parameters [17] that explore free-energy surfaces that are less accessible to non-adaptive strategies. In metadynamics [18] and expanded ensemble [19], simulations traverse different simulation states based on weights “learned” adaptively. Markov State Model [5] (MSM) approaches adaptively select starting configurations for simulations to reduce uncertainty of the resulting model.

Although adaptive ensemble algorithms are showing promising results, current solutions to encode and execute these algorithms fall into two categories: monolithic workflow systems that do not fully support adaptive algorithms and MD software packages where the adaptivity is embedded within the executing kernels. Exemplar workflow systems such as Kepler [20], Taverna [21], Pegasus [22], and several other workflow systems [23] support adaptation capabilities only as a form of fault tolerance and not as a way to enable decision-logic for changing the workflow at runtime.

MD software packages such as Amber [24], Gromacs [25] and NAMD [26] offer capabilities to execute multiple independent MD simulations, multi-dimensional replica exchange, steered MD simulations, adaptive biasing or metadynamics. However, these capabilities are tightly coupled to the MD code, preventing users from easily adding new adaptive algorithms.

Domain-specific workflow systems such as Copernicus [27] have also been developed to support Markov state modeling algorithms to study kinetics of bio-molecules. Although Copernicus provides an interactive and customized interface to domain scientists, it requires users to manage resources, the deployment of the system and the configuration of the execution environment. This hinders Copernicus uptake, often requiring tailored guidance from its developers.

Encoding the adaptive ensemble algorithm, including its adaptation logic within MD software packages or workflow systems binds the capabilities to those individual tools. In contrast, the capability to encode the algorithm and adaptation logic as an user application offers several benefits: separation between algorithm specification and execution; flexible and quick prototyping of different algorithms; and extensibility of algorithmic solutions to multiple science problems and domains [28].

In this paper, we develop abstractions and capabilities to encode and execute adaptive ensemble applications on HPC systems. We implement two exemplar science drivers from the biomolecular science domain to present how these abstractions can enable and accelerate distributed collaborative efforts towards explorative scientific methodologies, via rapid reuse and improvement of existing software frameworks.

## III. SCIENCE DRIVERS

Adaptive ensemble applications span several science domains including, but not limited to, climate science, seismology, astrophysics, and bio-molecular science. In Ref. [29] studies adaptive selection and tuning of dynamic RNNs for hydrological forecasting. Ref. [30] presents *atmos* for adaptive modeling of oceanic and atmospheric circulation. Ref. [31] studies adaptive

assessment methods on an ensemble of bridges subjected to earthquake motion. Ref. [32] discusses parallel adaptive mesh refinement techniques for astrophysical and cosmological applications. In this paper, we discuss two representative adaptive ensemble simulation algorithms from the biophysical domain: Expanded Ensemble and Markov State Modeling.

### A. Expanded Ensemble

Metadynamics [18] and expanded ensemble (EE) dynamics [19] are a class of bio-molecular algorithms, where, similar to replica exchange, individual simulations jump between simulation conditions. In EE dynamics, the simulation states take one of  $N$  discrete states of interest, whereas in metadynamics, the simulation states are described by one or more continuous variables. In contrast to replica exchange, the change of simulation conditions of each simulation is not directly coupled together, but instead each simulation explores states independently. Additional weights are required to force the simulations to visit desired distributions in simulation condition space, which usually involves sampling in all the simulation conditions. These weights are learned adaptively using a variety of schemes [19].

Since the movement between state spaces is essentially diffusive, the larger the simulation state spaces that are used, the more sampling is slowed down. This can be handled using “multiple walker” approaches, with more than one simulation exploring the same state space [33].

As discussed above, there are a number of adaptive choices in the methods for collectively building up the weights [19], [34]. Another choice of adaptivity includes partitioning the simulation condition range into individual simulations (smaller partitions decrease diffusive behavior [35], but the “best” partitions to spend time sampling may not be known until after simulation). Additionally, EE and metadynamics are far more adaptable to changes in the resources available than replica exchange, as the number of simulations can dynamically increase or decrease, and any choice of adaptivity can be much more asynchronous, as the need for collective exchange at set checkpoints required for replica exchange is eliminated.

In this paper, we implement two versions of the EE algorithm as an application consisting of concurrent, iterative ensemble members that analyze data at regular intervals. In the first version, EE with local analysis, we analyze data local to each ensemble member; while in EE with global analysis, the ensemble members asynchronously exchange data with other members. In our application, each ensemble member consists of two types of tasks: simulation and analysis. The simulation tasks generate MD trajectory data while the analysis tasks use this MD trajectory data, both current and historical, from individual or all ensemble members, depending on the analysis scope, to generate simulation condition weights for the next iteration of simulation in its own ensemble member. In this method, every analysis task operates on the current snapshot of the total local or global data. Note that in global analysis, EE uses any and all data available and does not ex-

plicitly “wait” for data from other ensemble members. Fig. 1 is a representation of this implementation.

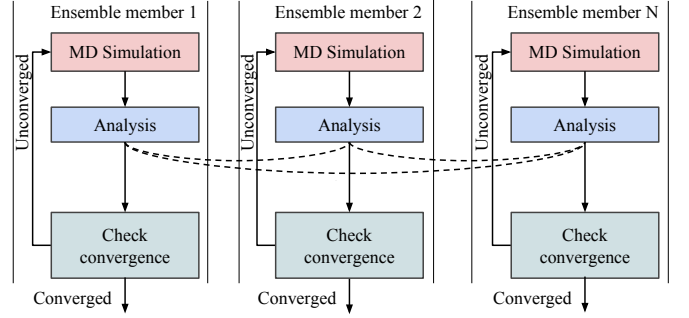


Fig. 1: Schematic of the expanded ensemble science driver.

### B. Markov State Modeling

Markov state modeling is another important class of simulation algorithms for determining kinetics of molecular models. Using an assumption of separation of time scales of molecular motion, the rates of first-order kinetic processes are learned adaptively. In a typical MSM simulation, a large ensemble of simulations, typically tens or hundreds of thousands, are run from different starting points, and similar configurations are clustered as states. The rates of transitions between these states are estimated by observing which entire kinetic behavior can then be inferred even though individual simulations perform no more than one state transition. However, the choice of where new simulations are initiated to best refine the definition of the states, improve the statistics of the rate constants, and discover new simulation states requires a range of analyses of previous methods, making the entire algorithm highly adaptive.

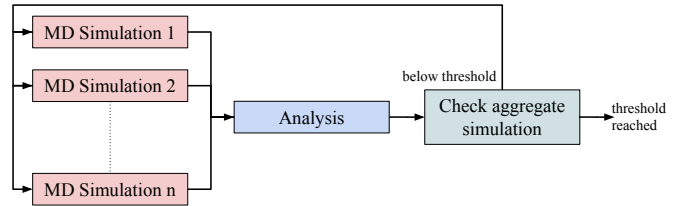


Fig. 2: Schematic of the Markov State Model science driver.

MSMs provide an attractive way to encode dynamic processes such as protein folding into a set of metastable states and transitions between them. In computing these models from simulation trajectories, the metastable state definitions and the transition probabilities have to be inferred. It has previously been shown [13], [14] that “adaptive sampling” can lead to more efficient MSM construction as follows: provisional models are constructed using intermediate simulation results, and these models are used to direct the placement of further simulation trajectories. This algorithm is encoded as an application consisting of an iterative pipeline with two stages: ensemble of simulations and MSM construction to determine optimal placement of future simulations. The first stage is repeated till sufficient amount of MD trajectory data is generated and analyzed. The analysis, i.e., second stage, operates over the

cumulative trajectory data to generate a new set of simulation configurations, used in the next iteration of the simulations. The pipeline is iterated until convergence of the resulting MSM. Fig. 2 is a representation of this application.

#### IV. WORKFLOW ADAPTIVITY

Ensemble-based applications involve a hierarchy of computational processes: at the lowest level is the specific simulation using an MD engine. An ensemble-based **algorithm** specifies an interaction (or lack thereof) among multiple MD simulations. The computational instance implementing an algorithm with specific parameter values, number of simulations and other computational aspects of that algorithm, constitutes a **workflow**. Typically, there is a one-to-many relationship between an algorithm and a workflow. A workflow may be fully specified a priori, or it may adapt one or more of its properties, say parameters, at runtime. We call the latter an adaptive workflow. We decompose the execution of adaptive workflows into four operations, discussing different types of adaptations and the abstractions they require.

##### A. Execution of Adaptive Workflows

Executing scalable and adaptive workflows on production-grade HPC resources, using ensemble-based methods presents several challenges [36]. For simplicity in the discussion of workflow adaptivity, we represent the workflow as a task-graph (TG) when discussing operations applied to the workflow. Workflow may be represented as multiple disjoint TGs. The following discussion regarding workflow adaptivity apply to other representations of a workflow.

Our analysis of adaptive workflows suggests that the complete TG is not known prior to execution and may change depending on intermediate runtime results. Execution of adaptive workflows can be decomposed into four operations as represented in Fig. 3: (a) creation of a TG by encoding its known portions; (b) traversal of a TG to identify tasks ready for execution in accordance with their dependencies; (c) execution of tasks on the compute resource; and (d) notification of completed tasks (control-flow) or generation of intermediate data (data-flow) which invokes adaptations of the TG.

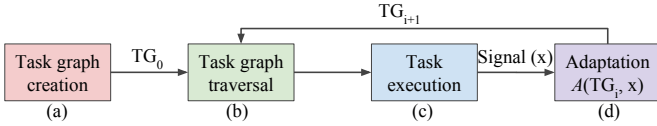


Fig. 3: **Adaptivity Loop**: Sequence of operations in executing an adaptive workflow

Operations (b)–(d) are repeated till the complete workflow is determined and all its tasks are executed. We call this sequence of operations an Adaptivity Loop and we use it to distinguish between adaptive and predefined workflows. In the former, the workflow “learns” its future state based on the execution of its current state; in the latter, the workflow is fully specified and only operations (a)–(c) are necessary.

Encoding of adaptive workflows requires two sets of abstractions: one to encode the workflow; and the other to encode the adaptation methods (A) that, upon receiving a signal  $x$ , operate

on the workflow. The former abstractions are required for creating the TG, i.e., operation (a), while the latter are required to adapt the TG, i.e., operation (d).

##### B. Types of Adaptations

The adaptation operation of the adaptivity loop (Fig. 3d) consists of applying an adaptation method to a TG. We represent the TG as  $TG = [V, E]$ , with a set of vertices  $V$ , denoting the tasks of the workflow and their properties (such as executable, required resources, and required data), and a set of directed edges  $E$ , denoting dependencies between these tasks. For a workflow with  $TG = [V, E]$ , there exist four parameters that may change during execution: (i) set of vertices; (ii) set of edges; (iii) size of the vertex set; and (iv) size of the edge set. We analyzed the  $16(2^4)$  permutations of these four parameters and identified 3 that are valid and unique. The remaining permutations represent conditions that are either not possible to achieve or combinations of the 3 valid permutations.

a) *Task-count adaptation*: We define a method  $A_{tc}$  (operator) as a task-count adaptation method if, on receiving a signal  $x$ , the method performs the following adaptation (operation) on the TG (operand):

$$TG_{i+1} = A_{tc}(TG_i, x) \implies size(V_i) \neq size(V_{i+1}) \wedge size(E_i) \neq size(E_{i+1})$$

where  $TG_i = [V_i, E_i]$  and  $TG_{i+1} = [V_{i+1}, E_{i+1}]$ . Task-count adaptation refers to the adaptation of the number of TG’s tasks, i.e., the adaptation method operates on a  $TG_i$  to produce a new  $TG_{i+1}$  such that at least one vertex and one edge is added or removed to/from  $TG_i$ .

b) *Task-order adaptation*: We define a method  $A_{to}$  as a task-order adaptation method if, on a signal  $x$ , the method performs the following adaptation on the TG:

$$TG_{i+1} = A_{to}(TG_i, x) \implies E_i \neq E_{i+1} \wedge V_i = V_{i+1}$$

where  $TG_i = [V_i, E_i]$  and  $TG_{i+1} = [V_{i+1}, E_{i+1}]$ . Task-order adaptation refers to the adaptation of the dependency order among tasks, i.e., the adaptation method operates on a  $TG_i$  to produce a new  $TG_{i+1}$  such that the vertices are unchanged but at least one of the edges between vertices is different between  $TG_i$  and  $TG_{i+1}$ .

c) *Task-property adaptation*: We define a method  $A_{tp}$  as a task-property adaptation method if, on a signal  $x$ , the method performs the following adaptation on the TG:

$$TG_{i+1} = A_{tp}(TG_i, x) \implies V_i \neq V_{i+1} \wedge size(V_i) = size(V_{i+1}) \wedge E_i = E_{i+1}$$

where  $TG_i = [V_i, E_i]$  and  $TG_{i+1} = [V_{i+1}, E_{i+1}]$ . Task-property adaptation refers to the adaptations in the properties of tasks, i.e., the adaptation method operates on a  $TG_i$  to produce a new  $TG_{i+1}$  such that the edges and the number of vertices are unchanged but the properties of at least one vertex is different between  $TG_i$  and  $TG_{i+1}$ .

We can represent the workflow of the two science drivers using the notations presented. Expanded ensemble consists of  $N$  ensemble members executing independently for multiple

iterations till convergence is reached in any ensemble member. We represent one iteration of each ensemble members as a task graph  $TG$  and the convergence criteria with  $x$ . Expanded ensemble workflow can then be represented as:

```
parallel_for i in [1 : N]:
  while (condition on x):
     $TG_i = A_{tp}(A_{to}(A_{tc}(TG_i)))$ 
```

Adaptive MSM consists of one ensemble member which iterates between simulation and analysis till sufficient trajectory data is analyzed. We represent one iteration of the ensemble member as a task graph  $TG$  and its termination criteria as  $x$ . Adaptive MSM workflow can then be represented as:

```
while (condition on x):
   $TG = A_{to}(A_{tc}(TG))$ 
```

### C. Challenges in Encoding Adaptive Workflows

Adaptive capabilities can be beneficial to domain science workflows but supporting them comes with three main challenges. The first challenge is the expressibility of adaptive workflows as their encoding requires APIs that enable the description of the initial state of the workflow and the specification of how the workflow adapts on the base of intermediate signals. The second challenge is determining when and how to instantiate the adaptation. Adaptation is described at the end of the execution of tasks wherein a new TG is generated. Different strategies can be employed for the instantiation of the adaptation [37]. The third challenge is in the implementation of the adaptation of the TG during runtime. We divide this challenge into three parts: (i) propagation of adapted TG to all components; (ii) consistency of the state of the TG among different components; and (iii) efficiency of adaptive operations.

## V. ENSEMBLE TOOLKIT

EnTK is an ensemble execution system, implemented as a Python library, that offers components to encode and execute ensemble workflows on HPC systems. EnTK decouples the description of ensemble workflows from their execution by separating three concerns: specification of tasks and resource requirements; resource selection and acquisition; and task execution management. EnTK sits between the user and the HPC system, abstracting resource management and execution management complexities from the user.

EnTK is developed based on requirements elicited by use cases spanning several scientific domains, including biomolecular sciences, climate sciences, and earth sciences. The design, implementation and performance of EnTK is discussed in detail in Ref. [38]. We present a schematic representation of EnTK in Fig. 4, summarize its design and implementation, and detail the enhancements made to EnTK to support the encoding and execution of the three adaptation types discussed in §IV-B.

### A. Design

EnTK exposes an API with three user-facing constructs: Pipeline, Stage, and Task, and one component, AppManager.

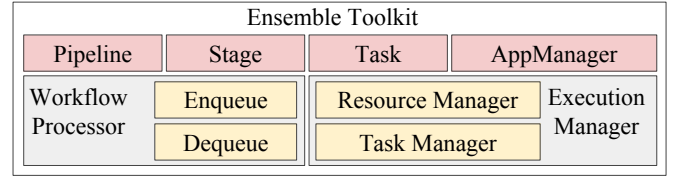


Fig. 4: Schematic of EnTK representing all its components and sub-components.

Pipeline, Stage, and Task constructs are used to encode the ensemble workflow in terms of concurrency and sequentiality of tasks. We define the constructs as:

- **Task:** an abstraction of a computational process consisting of the specification of the executable, software environment, resource and data requirement.
- **Stage:** a set of tasks without mutual dependencies that, therefore, can be concurrently executed.
- **Pipeline:** a sequence of stages such that any stage  $i$  can be executed only after stage  $i-1$ .

Ensemble workflows are described by the user as a set or sequence of pipelines, where each pipeline is a list of stages, and each stage is a set of tasks. A set of pipelines executes concurrently whereas a sequence executes sequentially. All the stages of each pipeline execute sequentially, and all the tasks of each stage execute concurrently. In this way, we describe a workflow in terms of the concurrency and sequentiality of tasks, without requiring explicit specifications of dependencies.

AppManager is the core component of EnTK that serves two broad purposes: (i) exposes an API to accept the encoded workflow and a specification of the resource requirements from the user, and (ii) manages the execution of the workflow on the specified resource via several components. AppManager abstracts complexities of resource acquisition, task and data management, heterogeneity, and failure handling from the user. All components and sub-components of EnTK communicate via a dedicated messaging system that is set up by the AppManager.

AppManager instantiates Workflow Processor, the component responsible for maintaining the concurrent and sequential execution of tasks as described by the pipelines and stages in the workflow. Workflow Processor consists of two components, Enqueue and Dequeue, that are used to enqueue sets of executable tasks, i.e., tasks with all their dependencies satisfied, and dequeue executed tasks to and from dedicated queues.

AppManager also instantiates Execution Manager, the component responsible for managing the resources and execution of the tasks on these resources. Execution Manager consists of two sub-components, Resource Manager and Task Manager, that interface with a runtime system (RTS) for managing allocation and deallocation of resources, and execution of sets of tasks, received via dedicated queues, respectively.

EnTK manages failures of tasks, components, computing infrastructure (CI) and RTS. Failed tasks can be resubmitted or ignored, depending on user configuration. AppManager holds the global state of all the stateful objects, i.e., pipelines, stages, and tasks. EnTK, by design, is resilient against component



failures as all state updates are transactional and failed components can simply be re-instantiated. Both the CI and RTS are considered black boxes and partial failures of their subcomponents at runtime are assumed to be handled locally. Upon full failure of the CI or RTS, EnTK assumes all the resources and the tasks undergoing execution are lost. EnTK starts a new instance of the RTS, acquires new set of resources, and resumes execution from the last successful pipelines, stages and tasks.

### B. Implementation

EnTK is implemented in Python, uses the RabbitMQ message queuing system [39] and the RADICAL-Pilot (RP) [40] RTS. All EnTK components are implemented as processes, and all subcomponents as threads. AppManager is the master process spawning all the other processes. Tasks, stages and pipelines are implemented as objects, copied among processes and threads via queues and transactions. Synchronization among processes is achieved by message-passing via queues.

Using RabbitMQ offers several benefits: (i) producers and consumers do not need to be topology-aware because they interact only with the server; (ii) messages are stored in the server and can be recovered upon failure of EnTK components; (iii) messages can be pushed and pulled asynchronously because data can be buffered by the server upon production; and (iv) up to at least  $O(10^6)$  tasks are supported.

EnTK uses RADICAL Pilot, a pilot system, as the RTS. Pilot systems enable the submission of container jobs to the resource manager of an HPC system. Once scheduled, the container job is used to execute the workflow tasks without requiring for each task to be queued on the HPC system. RP does not attempt to ‘game’ the resource manager of the HPC system: Once queued, the resources are managed according to the system’s policies. RP provides interoperable access to several HPC systems, including XSEDE, ORNL, and NCSA resources. RP can be configured to use other HPC systems by integrating their queue and access policy details.

### C. Enhancements for Adaptive Execution

In §IV-C, we described three challenges for supporting adaptive workflows: expressibility, instantiation and implementation of adaptive operations. EnTK cannot support adaptive workflows with the capabilities described above as there are no means to express adaptation requirements and algorithms. Therefore, we enhanced EnTK with three new capabilities to address these challenges: expressing an adaptation operation, executing that operation and modifying a TG at runtime.

Adaptations in ensemble workflows follow the adaptivity loop as described in §IV-A. Execution of one or more tasks is followed by some signal  $x$  that triggers an adaptation operation. We added the capability to express this adaptation operation as a post-condition of stages and pipelines. In this way, when all the tasks of a stage or all the stages of a pipeline have been completed, the adaptation operation can be used to evaluate whether a change in the TG is required, based on the results of the ongoing computation.

The adaptation operation is encoded as a Python attribute of the Stage and Pipeline objects. The encoding requires the specification of three functions: one function to evaluate a boolean condition over  $x$ , and two functions describing the adaptation, depending on the result of the boolean evaluation.

Ref. [37] specifies multiple strategies to perform adaptation: forward recovery, backward recovery, proceed, and transfer. In EnTK, we implement a non-aggressive adaptation strategy, similar to ‘transfer’, where a new TG is created by extending the current TG only after the completion of part of that TG. The choice of this strategy is based on the current science drivers where tasks that have already executed and tasks that are currently executing are not required to be adapted but all forthcoming tasks might be.

Modifying the TG at runtime requires coordination among EnTK components to ensure consistency in TG representation. AppManager holds the global view of the TG and, upon instantiation, Workflow Processor maintains a local copy of that TG. The dequeue sub-component of Workflow Processor acquires a lock over the local copy of the TG, and invokes the adaptation operation as post-condition of stages and pipelines. If changes to the TG are required, Workflow Processor transmits those changes to AppManager that modifies the global copy of TG, and releases the lock upon receiving an acknowledgment. This mechanism ensures that the adaptations to the TG are consistent across all components, requiring minimal communication across components.

Pipeline, stage and task descriptions alongside the specification of an adaptation operation as post-condition for pipelines and stages enable the expression of adaptive workflows. The ‘transfer’ strategy enacts the adaptivity of the TG, and the implementation in EnTK ensures consistency and minimal communication in executing adaptive workflows.

## VI. EXPERIMENTS

We perform five experiments to characterize three types of adaptation overhead of EnTK: task-count, task-order, and task-property. We implement the two science drivers presented in § III with EnTK and validate these implementations by comparing their results against reference data. Lastly, we perform four production scale experiments to evaluate the results of EE with local and global analysis, and compare against results obtained by a single and an ensemble of MD simulations.

We use three application kernels in our experiments: `stress-ng` [41], `GROMACS` [25], and Python scripts. `stress-ng` allows to control the computational duration of a task for the experiments that characterize the adaptation overhead of EnTK, while `GROMACS` and `OpenMM` are the simulation kernels for the EE and MSM experiments respectively. We validate our implementation of EE by calculating the binding of the cucurbit[7]uril 6-ammonio-1-hexanol host-guest system, and our implementation of MSM by simulating the Alanine dipeptide system and comparing our results with the reference data of the DESRES group [42].

We executed all experiments from the same host machine but we targeted three HPC systems, depending on the amount and

availability of the resources required by the experiments, and the constraints imposed by the queue policy of each machine. NCSA Blue Waters and ORNL Titan were used for characterizing the adaptation overhead of EnTK, while XSEDE SuperMIC was used for the validation and production scale experiments.

#### A. Characterization of Adaptation Overhead

We perform five experiments to characterize the overhead of adapting workflows encoded using EnTK. Each experiment measures the overhead of a type of adaptation as a function of the number of adaptations. In the case of task-count adaptation, the overhead is measured also as a function of the number of tasks and of their type: single-node and multi-node. This is relevant because with the growing of the size of the simulated molecular system and of the duration of that simulation, multi-node tasks may perform better than single-node ones.

Each experiment measures the EnTK Adaptation Overhead and the Task Execution Time. The former is the time taken by EnTK to adapt the workflow by invoking the user-specified algorithms; the latter is the time taken to run the executables of all tasks of the workflow. Consistent with the scope of this paper, the comparison between each adaptation overhead and the workflow execution time offers a measure of the efficiency with which EnTK implements adaptive functionalities. Ref. [38] offers a detailed analysis of other types of overheads.

Table I describes the variables and fixed parameters of the five experiments. In these experiments, the algorithm is encoded in EnTK as 1 pipeline consisting of several stages with a set of tasks. In task-count adaptation experiments (i–iii), the pipeline initially consists of a single stage with 16 tasks of a certain type. Each adaptation, occurring upon the completion of a stage, adds 1 stage with a certain number of tasks of a certain type, thereby increasing the task-count in the workflow.

In the task-order (iv) and task-property (v) adaptation experiments, the workflow is encoded as 1 pipeline with 17, 65, or 257 stages with 16 tasks per stage. Each adaptation occurs upon the completion of a stage and, in the case of task-order adaption, the remaining stages of the pipeline are shuffled; in the case of task-property adaption, the number of cores used by the tasks of the next stage is set to a random value below 16, keeping the task type to single-node. The last stage of both experiments is non-adaptive, resulting in 16, 64, and 256 task-order and task-property adaptations.

In each experiment in which the number of adaptations vary (i, iv, v), each task of the workflow executes the `stress-ng` kernel for 60 seconds. For experiments with  $O(1000)$  tasks (ii, iii), the execution duration is set to 600 seconds so to avoid performance bottlenecks in the underlying RTS and potential interferences with the measurement of EnTK adaptation overheads. All experiments have no data movement as the performance of data operations is independent from that of adaptation.

In Fig. 5 (i, iv, v), EnTK Adaptation Overhead and Task Execution Time increase linearly with the increasing of the number of adaptations. The increase in the overhead is explained by the time taken to compute the additional adaptations, while

its linearity indicates that the time taken by computing each adaptation is constant. The increase in Task Execution Time is explained by the time taken to execute the tasks of the stages that are added to the workflow as result of the adaptation.

Fig. 5 (i, iv, v) also show that task-property adaptation (v) is the most expensive, followed by task-order adaptation (iv) and task-count (i) adaptation. These differences depend on the computational cost of the Python functions executed during adaptation: in (v), the function parses the entire workflow and invokes the Python `random.randint` function 16 times per adaptation; in (iv), the Python function shuffles a Python list of stages; and in (i), the Python function creates a stage, appending it to a list.

In Fig. 5 (ii), EnTK Adaptation Overhead increases linearly with an increase in the number of tasks added per task-count adaptation, explained by the cost of creating additional tasks and adding them to the workflow. The Task Execution Time remains constant at  $\approx 1200$ s, since sufficient resources are acquired to execute all the tasks concurrently.

Fig 5 (iii) compares EnTK Adaptation Overhead and Task Execution Time when adding single-node and multi-node tasks to the workflow. The former is greater by  $\approx 1$ s when adding multinode tasks, whereas the latter remains constant at  $\approx 1200$ s in both scenarios. The difference in the overhead, although negligible when compared to Task Execution Time, is explained by the increased size of a multi-node task description. As in (ii), Task Execution Time remains constant due to acquisition of sufficient resources to execute all tasks concurrently.

Experiments (i–v) show that EnTK Adaptation Overhead is proportional to the computing required by the adaptation algorithm and is not determined by the design or implementation of EnTK. In absolute terms, EnTK Adaptation Overhead is orders of magnitude smaller than Task Execution Time. EnTK, thus, takes a step forward in bringing the concepts of workflow adaptivity to practical use.

#### B. Validation of Science Driver Implementations

We implement the two science drivers using the abstractions developed in EnTK. We validate the scientific results obtained from executing these implementations against a reference calculation and a published dataset.

1) *Expanded Ensemble*: We execute the EE science driver described in § III-A on XSEDE SuperMIC for an aggregate simulation time of 2270ns. To validate the process, we carry out a set of simulations of the binding of cucurbit[7]uril (host) to 6-amino-1-hexanol (guest) in explicit solvent for a total of 29.12ns per ensemble member, and compare the final free energy estimate to a reference calculation. Each ensemble member is encoded as a pipeline of stages of simulation and analysis tasks in EnTK with each pipeline using 1 node for 72 hours. With 16 ensemble members for the current physical system, we use 23K core-hours of computation resources.

The expanded ensemble variable is the degree of coupling between the guest and the rest of the system (water and host). As the system explores this coupling variable using EE dynamics, it is able to unbind and bind to the host. The free

TABLE I: Parameters of the experiments plotted in Fig. 5

ID	Adaptation Type	Experiment variable	Fixed parameters
i	Task-count	Number of adaptations	Number of tasks added per adaptation = 16, Type of tasks added = single-node
ii	Task-count	Number of tasks added per adaptation	Number of adaptations = 2, Type of tasks added = single-node
iii	Task-count	Type of tasks added	Number of adaptations = 2, Number of tasks added per adaptation = $2^{10} * 2^s$ ( $s$ =stage index)
iv	Task-order	Number of adaptations	Number of re-ordering operations per adaptation = 1, Type of re-ordering = uniform shuffle
v	Task-property	Number of adaptations	Number of property modified per adaptation = 1, Property adapted = Number of cores used per task

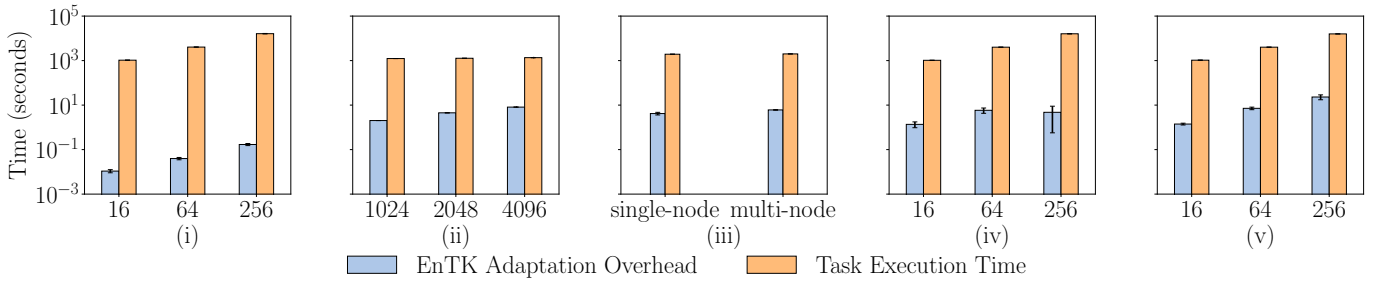


Fig. 5: EnTK Adaptation Overhead and Task Execution Time for task-count (i, ii, and iii), task-order (iv), and task-property (v) adaptations.

energy of this process is gradually estimated over the course of the simulation using the Wang-Landau (WL) algorithm [43]. However, we hypothesize we can speed convergence by allowing parallel simulations to share information with each other, and estimate the free energies using the potential energy differences among states with the Multistate Bennett Acceptance Ratio (MBAR) algorithm [44].

Four approaches to communication among the ensemble members are:

- **Method 1:** one continuous simulation (omitting *any* intermediate analysis).
- **Method 2:** multiple parallel simulations without any intermediate analysis.
- **Method 3:** multiple parallel simulations with local analysis, i.e., using current and historical simulation information from only its own ensemble member. This eliminates any effects caused by the intermediate analysis, providing a better estimate of the weights than the WL algorithm.
- **Method 4:** multiple parallel simulations with global analysis, i.e., using current and historical simulation information from all ensemble members.

In each method, the latter 2/3 of the simulation data available at the time of each analysis is used for free energy estimates using MBAR. In cases where intermediate analysis is used to update the weights, the intermediate analysis is always applied at 320ps intervals.

The reference calculation consisted of four parallel simulations that ran for 200ns each and with fixed weights, i.e., using

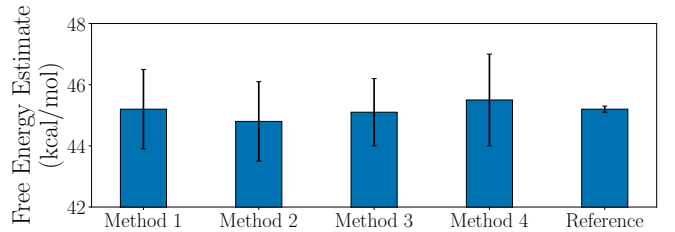


Fig. 6: Validation of expanded ensemble implementation: Observed variation of free energy estimate for methods 1–4. Reference is the MBAR estimate and standard deviation of four 200ns fixed weight expanded-ensemble simulations.

a set of estimated weights and not using the Wang-Landau algorithm. MBAR was used to estimate the free energy for each of these simulations. The reference value is reported as the MBAR estimate of the pooled reference data and its error is reported as the standard deviation of the non-pooled MBAR estimates. Weights used in these fixed weight simulations were estimated by running MBAR on data generated by a 400ns Wang-Landau algorithm expanded ensemble simulation.

Free energy estimates obtained through each of the four methods are plotted with the reference calculations value in Fig. 6. Final estimates of each method agree within error to the reference values, validating that the adaptive ensemble based approaches converge the free energy estimate to the true value.

2) *Markov State Modeling:* We execute the MSM science driver described in § III-B on XSEDE SuperMIC for an aggre-



gate simulation time of 100ns over multiple iterations. Each iteration of the task graph is encoded in EnTK as one pipeline with 2 stages consisting of 10 simulation tasks and 1 analysis task. Each task uses 1 node to simulate 1ns.

We compare the results obtained from execution of the EnTK implementation against reference data by performing the clustering of the reference data and deriving the mean eigenvalues of two levels of the metastable states, i.e., macro- and micro-states. The reference data was generated by a non-adaptive workflow consisting of 10 tasks, each simulating 10ns.

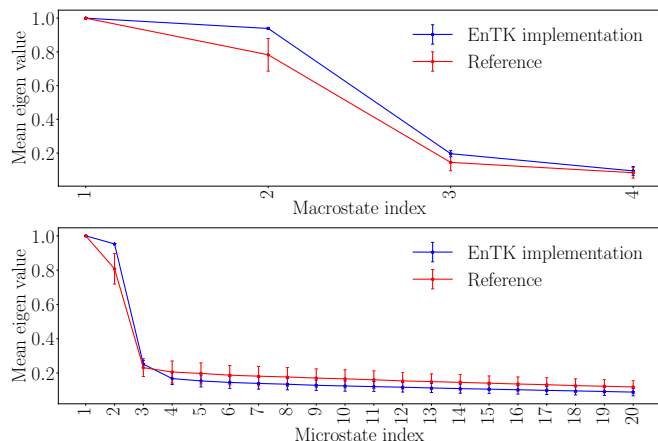


Fig. 7: Mean eigenvalue attained by the macro-states (top) and micro-states (bottom) by Alanine dipeptide after aggregate simulation duration of 100ns implemented using EnTK compared against reference data.

Eigen values attained by the macro-states (top) and micro-states (bottom) in the EnTK implementation and reference data are plotted as a function of the state index in Fig. 7. Final eigenvalues attained by the implementation agree with the reference data within the error bounds. The validation of the implementation warrants that similar implementations should be investigated for larger molecular systems and longer durations, where the aggregate duration is unknown and termination conditions are evaluated during runtime.

### C. Expanded Ensemble at Scale

We analyzed the convergence properties of the free energy estimate using the data generated for validation. MBAR was used to estimate the free energy difference of cucurbit[7]uril (host) 6-amino-1-hexanol (guest) binding as a function of total simulation time available per ensemble member, using the latter 2/3 of the simulation data. This data is plotted for each method, as well as the reference calculation, in Fig. 8. The convergence behavior of Method 1 observed in Fig. 8 implies that the current method converges faster than ensemble based methods but does not represent the average behavior of the non-ensemble based approach. The average behavior is depicted more clearly by Method 2 because this method averages the free energy estimate of 16 independent single simulations.

The most significant feature of Fig. 8 is that all three ensemble based methods converge at similar rates to the reference

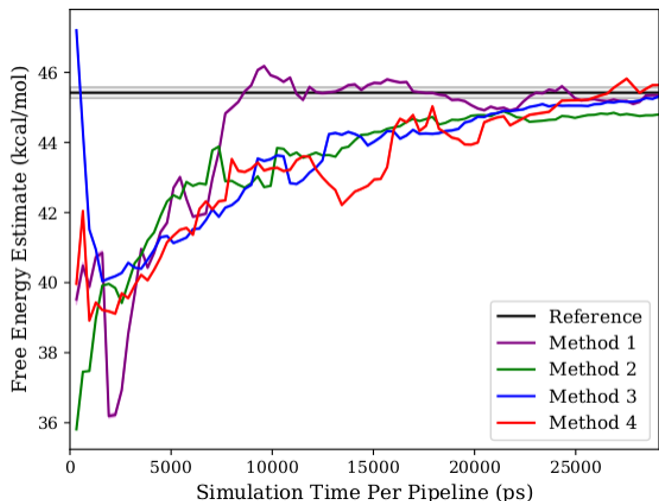


Fig. 8: Convergence of expanded ensemble implementation: Observed convergence behavior in methods 1–4. Reference is the MBAR estimate of the pooled data and the standard deviation of the non-pooled MBAR estimates of four 200ns fixed weight expanded ensemble simulations.

value. We initially hypothesized that adding adaptive analysis to the estimate of the weights would improve convergence behavior but we see no significant change in these experiments. However, the methodology described here gives researchers the ability to implement additional adaptive elements and test their effects on system properties. Additionally, these adaptive elements can be implemented on relatively short time scales, giving the ability to test many implementations.

Analysis of these simulations revealed a fundamental physical reason that demonstrates a need for additional adaptivity to successfully accelerate these simulations. Although expanded ensemble simulations allowed the ligand to move in and out of the binding pocket rapidly, the slowest motion, occurring on the order of 10's of nanoseconds, was the movement of water out of the binding pocket, allowing the ligand to bind as water backs into a vacant binding pocket. Simulation biases that equilibrate on shorter timescales may stabilize either the waters out or the waters in configurations, preventing the sampling of both configurations. Additional biasing variables are needed to accelerate this slow motions, algorithmically requiring a combination of metadynamics and expanded ensemble simulations, with biases both in the protein interaction variable, and the collective variable of water occupancy in the binding pocket. Changes in the PLUMED2 [45] metadynamics code are being coordinated with the developers to make this possible.

Analysis of the slow motions of the system suggests the potential power of more complex and general adaptive patterns. Simulations with accelerated dynamics along the hypothesized degrees of freedom can be carried out, and resulting dynamics can be analyzed, automated and monitored for degrees of freedom associated with remaining slow degrees of motion [46]. Accelerated dynamics can be adaptively adjusted as the simulation process continues. Characterization experiments suggest that EnTK can support the execution of this enhanced adaptive

workflow with minimal overhead.

## VII. CONCLUSION

Scientific problems across domains such as biomolecular science, climate science and uncertainty quantification require ensembles of computational tasks to achieve a desired solution. Novel approaches focus on adaptive algorithms that leverage intermediate data to study larger problems, longer time scales and to engineer better fidelity in the modeling of complex phenomena. In this paper, we described the operations in executing adaptive workflows, classified the different types of adaptations, and described challenges in implementing them in software tools. We enhanced EnTK to support the execution of adaptive workflows on HPC systems. We characterized the adaptation overhead in EnTK, validated the implementation of the two science drivers and executed EE at production scale and evaluated its sampling capabilities. To the best of our knowledge, this is the first attempt at describing and implementing multiple adaptive ensemble workflows using a common conceptual and implementation framework.

## REFERENCES

- [1] T. Cheatham and D. Roe, "The impact of heterogeneous computing on workflows for biomolecular simulation and analysis," *Computing in Science and Engineering*, vol. 17, no. 2, pp. 30–39, 3 2015.
- [2] J. Comer, J. C. Phillips, K. Schulten, and C. Chipot, "Multiple-replica strategies for free-energy calculations in namd: multiple-walker adaptive biasing force and walker selection rules," *Journal of chemical theory and computation*, vol. 10, no. 12, pp. 5276–5285, 2014.
- [3] A. Laio and M. Parrinello, "Escaping free-energy minima," *Proc. Natl. Acad. Sci. USA*, vol. 99, no. 20, Oct. 2002.
- [4] L. Maragliano, B. Roux, and E. Vanden-Eijnden, "Comparison between mean forces and swarms-of-trajectories string methods," *Journal of chemical theory and computation*, vol. 10, no. 2, pp. 524–533, 2014.
- [5] J. D. Chodera, W. C. Swope, J. W. Pitera, and K. A. Dill, "Long-time protein folding dynamics from short-time molecular dynamics simulations," *Multiscale Modeling & Simulation*, vol. 5, no. 4, pp. 1214–1226, 2006.
- [6] B. E. Husic and V. S. Pande, "Markov state models: From an art to a science," *J. Am. Chem. Soc.*, vol. 140, no. 7, pp. 2386–2396, 2018.
- [7] C. Abrams and G. Bussi, "Enhanced sampling in molecular dynamics using metadynamics, replica-exchange, and temperature-acceleration," *Entropy*, vol. 16, no. 1, pp. 163–199, 2014.
- [8] G. R. Bowman, D. L. Ensign, and V. S. Pande, "Enhanced modeling via network theory: Adaptive sampling of markov state models," *Journal of Chemical Theory and Computation*, vol. 6, no. 3, pp. 787–794, 2010.
- [9] D. E. Shaw, M. M. Deneroff, R. O. Dror, J. S. Kuskin, R. H. Larson, J. K. Salmon *et al.*, "Anton, a special-purpose machine for molecular dynamics simulation," *Communications of the ACM*, vol. 51, no. 7, pp. 91–97, 2008.
- [10] Y. Komeiji, M. Uebayasi, R. Takata, A. Shimizu, K. Itsukashi, and M. Taiji, "Fast and accurate molecular dynamics simulation of a protein using a special-purpose computer," *Journal of Computational Chemistry*, vol. 18, no. 12, pp. 1546–1563, 1997.
- [11] H. A. Atwater and A. Polman, "Plasmonics for improved photovoltaic devices," *Nat. Mater.*, vol. 9, pp. 205–213, 2010.
- [12] S. Napolitano, E. Glynos, and N. B. Tito, "Glass transition of polymers in bulk, confined geometries, and near interfaces," *Rep. Prog. Phys.*, vol. 80, no. 3, MAR 2017.
- [13] N. S. Hinrichs and V. S. Pande, "Calculation of the distribution of eigenvalues and eigenvectors in markovian state models for molecular dynamics," *The Journal of chemical physics*, vol. 126, no. 24, p. 244101, 2007.
- [14] N. Singhal and V. S. Pande, "Error analysis and efficient sampling in markovian state models for molecular dynamics," *The Journal of chemical physics*, vol. 123, no. 20, p. 204909, 2005.
- [15] A. Mitsutake and Y. Okamoto, "Replica-exchange extensions of simulated tempering method," *The Journal of chemical physics*, vol. 121, no. 6, pp. 2491–2504, 2004.
- [16] Y. Okamoto, "Generalized-ensemble algorithms: enhanced sampling techniques for monte carlo and molecular dynamics simulations," *Journal of Molecular Graphics and Modelling*, vol. 22, no. 5, pp. 425–439, 2004.
- [17] V. Babin, C. Roland, and C. Sagui, "Adaptively biased molecular dynamics for free energy calculations," *The Journal of chemical physics*, vol. 128, no. 13, p. 134101, 2008.
- [18] A. Barducci, M. Bonomi, and M. Parrinello, "Metadynamics," *Wiley Interdiscip. Rev. Comput. Mol. Sci.*, vol. 1, no. 5, pp. 826–843, Sep. 2011. [Online]. Available: <http://doi.wiley.com/10.1002/wcms.31>
- [19] R. Chelli and G. F. Signorini, "Serial Generalized Ensemble Simulations of Biomolecules with Self-Consistent Determination of Weights," *J. Chem. Theory Comput.*, vol. 8, no. 3, pp. 830–842, Mar. 2012.
- [20] S. Bowers, B. Ludascher, A. H. Ngu, and T. Critchlow, "Enabling scientific workflow reuse through structured composition of dataflow and control-flow," in *Data engineering workshops, 2006. proceedings. 22nd international conference on.* IEEE, 2006, pp. 70–70.
- [21] P. Missier, S. Soiland-Reyes, S. Owen, W. Tan, A. Nenadic, I. Dunlop *et al.*, "Taverna, reloaded," in *International conference on scientific and statistical database management.* Springer, 2010, pp. 471–481.
- [22] T. Samak, D. Gunter, M. Goode, E. Deelman, G. Mehta, F. Silva, and K. Vahi, "Failure prediction and localization in large scientific workflows," in *Proceedings of the 6th workshop on Workflows in support of large-scale science.* ACM, 2011, pp. 107–116.
- [23] M. Mattoso, J. Dias, K. A. Ocaña, E. Ogasawara, F. Costa, F. Horta *et al.*, "Dynamic steering of hpc scientific workflows: A survey," *Future Generation Computer Systems*, vol. 46, pp. 100–113, 2015.
- [24] D. A. Case, T. E. Cheatham, T. Darden, H. Gohlke, R. Luo, K. M. Merz *et al.*, "The amber biomolecular simulation programs," *Journal of computational chemistry*, vol. 26, no. 16, pp. 1668–1688, 2005.
- [25] M. J. Abraham, T. Murtola, R. Schulz, S. Páll, J. C. Smith, B. Hess, and E. Lindahl, "Gromacs: High performance molecular simulations through multi-level parallelism from laptops to supercomputers," *SoftwareX*, vol. 1, pp. 19–25, 2015.
- [26] J. C. Phillips, R. Braun, W. Wang, J. Gumbart, E. Tajkhorshid, E. Villa *et al.*, "Scalable molecular dynamics with namd," *Journal of computational chemistry*, vol. 26, no. 16, pp. 1781–1802, 2005.
- [27] S. Pronk, I. Pouya, M. Lundborg, G. Rotskoff, B. Wesen, P. M. Kasson, and E. Lindahl, "Molecular simulation workflows as parallel algorithms: The execution engine of copernicus, a distributed high-performance computing platform," *Journal of chemical theory and computation*, vol. 11, no. 6, pp. 2600–2608, 2015.
- [28] P. K. McKinley, S. M. Sadjadi, E. P. Kasten, and B. H. Cheng, "Composing adaptive software," *Computer*, vol. 37, no. 7, pp. 56–64, 2004.
- [29] P. Coulibaly and C. K. Baldwin, "Nonstationary hydrological time series forecasting using nonlinear dynamic methods," *Journal of Hydrology*, vol. 307, no. 1–4, pp. 164–174, 2005.
- [30] J. Behrens, N. Rakowsky, W. Hiller, D. Handorf, M. L  uter, J. P  pke *et al.*, "amatos: Parallel adaptive mesh generator for atmospheric and oceanic simulation," *Ocean Modelling*, vol. 10, no. 1–2, pp. 171–183, 2005.
- [31] C. Casarotti and R. Pinho, "An adaptive capacity spectrum method for assessment of bridges subjected to earthquake action," *Bulletin of Earthquake Engineering*, vol. 5, no. 3, pp. 377–390, 2007.
- [32] Z. Lan, V. E. Taylor, and G. Bryan, "Dynamic load balancing for structured adaptive mesh refinement applications," in *Parallel Processing, 2001. International Conference on.* IEEE, 2001, pp. 571–579.
- [33] J. Comer, J. C. Phillips, K. Schulten, and C. Chipot, "Multiple-Replica Strategies for Free-Energy Calculations in NAMD: Multiple-Walker Adaptive Biasing Force and Walker Selection Rules," *J. Chem. Theory Comput.*, vol. 10, no. 12, pp. 5276–5285, Dec. 2014.
- [34] J. D. Chodera and M. R. Shirts, "Replica exchange and expanded ensemble simulations as Gibbs sampling: simple improvements for enhanced mixing," *J. Chem. Phys.*, vol. 135, no. 19, p. 194110, Nov. 2011.
- [35] L. Janosi and M. Doxastakis, "Accelerating flat-histogram methods for potential of mean force calculations," *J. Chem. Phys.*, vol. 131, no. 5, p. 054105, Aug. 2009.
- [36] P. M. Kasson and S. Jha, "Adaptive ensemble simulations of biomolecules," *Current opinion in structural biology*, vol. 52, pp. 87–94, 2018.
- [37] W. M. van der Aalst and S. Jablonski, "Dealing with workflow change: identification of issues and solutions," *Computer systems science and engineering*, vol. 15, no. 5, pp. 267–276, 2000.
- [38] V. Balasubramanian, M. Turilli, W. Hu, M. Lefebvre, W. Lei, R. T. Modrak, G. Cervone, J. Tromp, and S. Jha, "Harnessing the power of many: Extensible toolkit for scalable ensemble applications," in *2018 IEEE International Parallel and Distributed Processing Symposium, IPDPS 2018, Vancouver, BC, Canada, May 21-25, 2018*, 2018, pp. 536–545.
- [39] "Rabbitmq," <https://www.rabbitmq.com/> (accessed March 2018).
- [40] A. Merzky, M. Turilli, M. Maldonado, M. Santeroos, and S. Jha, "Using pilot systems to execute many task workloads on supercomputers," 2018, (under review) <http://arxiv.org/abs/1512.08194>.
- [41] "Stress-ng," <http://kernel.ubuntu.com/~cking/stress-ng/stress-ng.pdf> (accessed March 2018).
- [42] "Md trajectories of ala2," [https://figshare.com/articles/new\\_fileset/1026131](https://figshare.com/articles/new_fileset/1026131) (accessed March 2018).
- [43] F. Wang and D. P. Landau, "Efficient, multiple-range random walk algorithm to calculate density of states," *Phys. Rev. Lett.*, vol. 86, pp. 2050–2053, 2001.
- [44] M. R. Shirts and J. D. Chodera, "Statistically optimal analysis of samples from multiple equilibrium states," *J. Chem. Phys.*, vol. 129, p. 124105, 2008.
- [45] G. A. Tribello, M. Bonomi, D. Branduardi, C. Camilloni, and G. Bussi, "Plumed 2: New feathers for an old bird," *Comput. Phys. Comm.*, vol. 185, no. 2, pp. 604 – 613, 2014.
- [46] P. Tiwary and B. J. Berne, "Spectral gap optimization of order parameters for sampling complex molecular systems," *Proceedings of the National Academy of Sciences*, 2016.